STM JOURNALS

Journal of
Remote Sensing & GIS

ISSN: 2230-7990 (Online)
ISSN: 2321-421X (Print)
Volume 16, Issue 3, 2025
September–December
DOI (Journal): 10.37591/JoRSG

https://journals.stmjournals.com/jorsg

Research JoRSG

Study of a Western Disturbance of 2023 Using Satellite-Based Observation, Reanalysis Data, and Numerical Simulation

Janvi Patel*[1], Nishtha Ahuja[2], Charu Singh[3]

Abstract

Western Disturbances (WDs) are synoptic-scale, extratropical storm systems that influence winter precipitation across northwest India. This study focuses on a specific WD event that occurred from 24–25 March 2023, affecting Jammu & Kashmir, Himachal Pradesh, Uttarakhand, and Punjab. The analysis integrates satellite observations, ERA-5 reanalysis data, and simulations from the Weather Research and Forecasting (WRF) model to evaluate the model's performance. The novelty of this study lies in its event-specific analysis of a recent WD and in quantifying the model's predictive accuracy over complex Himalayan terrain. The WRF model effectively captures snowfall (RMSE: 1.40 mm), U10 wind (RMSE: 0.63 m/s), and V10 wind (RMSE: 0.30 m/s), but underperforms significantly for rainfall (RMSE: 4.46 mm). Time-series analysis reveals inverse relationships between total cloud cover and outgoing longwave radiation (OLR), and between snowfall and wind speed, consistent with expected meteorological dynamics. These findings highlight the strengths and limitations of mesoscale numerical modeling for WD forecasting. The study underscores the need for improved rainfall simulation techniques in complex terrains and supports the integration of high-resolution models for better regional forecasting, agricultural planning, and disaster management.

Keywords: Western disturbance, Northwest India, WRF model, satellite observation, ERA-5, model validation

INTRODUCTION

Western Disturbances (WDs) are synoptic-scale, mid-latitude systems that originate over the Mediterranean region and travel eastward under the influence of the subtropical westerly jet stream [1]. These disturbances are the major source of non-monsoonal precipitation in northwestern India, particularly affecting states such as Jammu & Kashmir, Himachal Pradesh, Uttarakhand, and Punjab [2]. Their wintertime precipitation is crucial for agricultural irrigation, replenishing water resources, and maintaining snowpack in the Himalayas [3].

Simulating WDs accurately remains a challenge for numerical weather prediction (NWP) models due to the region's rugged terrain, sparse *in-situ* observations, and limitations in model physics [4, 5]. The Weather Research and Forecasting (WRF) model, widely used for regional applications, often

***Author for Correspondence**
Janvi Patel
E-mail: janvipatel4818@gmail.com

[1-2]Master's Student, Dhirubhai Ambani Institute of Information & Communication Technology, Gandhinagar, Gujarat, India
[3]Scientist/Engineer, SF Marine and Atmospheric Science Department, Indian Institute of Remote Sensing, ISRO, Govt. of India, 4, Kalidas Road, Uttarakhand, India

Received Date: July 22, 2025
Accepted Date: July 28, 2025
Published Date: September 08, 2025

Citation: Janvi Patel. Study of a Western Disturbance of 2023 Using Satellite-Based Observation, Reanalysis Data, and Numerical Simulation. Journal of Remote Sensing & GIS. 2025; 16(3): 16–38p.

underestimates rainfall or misrepresents its spatial distribution during WD events [6]. While much of the existing literature focuses on climatology or multi-year WD trends, there is a noticeable gap in high-resolution, event-specific evaluations. To provide context, Table 1 summarizes commonly used global and regional models for atmospheric forecasting, outlining their resolution, forecast range, and strengths.

India's meteorological infrastructure is led by the India Meteorological Department (IMD), which categorizes weather by four major seasons. WDs typically impact the region during winter (December–April), with effects ranging from beneficial snow and rain to damaging floods, landslides, and crop loss [7].

Recently, the combination of remote sensing and data science has enhanced weather monitoring and disaster risk assessment. Applications of machine learning (ML) and deep learning (DL) are expanding rapidly, with use cases in flood prediction [8], deformation monitoring [9] Crop damage assessment [10], and pollution analysis [11]. However, their integration with mesoscale weather models like WRF, especially for event-scale WD simulations remains underutilized.

This study focuses on the 24–25 March 2023 Western Disturbance, which had measurable impacts across the northwest Indian region (Figure 1). High-resolution WRF simulations are validated using ERA-5 reanalysis and satellite datasets (INSAT-3D, PERSIANN) to evaluate the model's performance in simulating key atmospheric parameters.

STUDY AREA

The present study encompasses the northwestern Indian states of Jammu & Kashmir, Himachal Pradesh, Uttarakhand, Punjab, Haryana, Delhi, and parts of northern Rajasthan, regions that lie directly in the trajectory path of Western Disturbances (WDs) as they migrate from the Mediterranean through Afghanistan and Pakistan into India. This geographical selection is scientifically strategic, as each state represents distinct topographic and climatic zones influenced uniquely by WD systems, particularly in March, when WD activity peaks in this region.

- Jammu & Kashmir and Himachal Pradesh, located in the western Himalayan region, serve as the first orographic barriers to incoming WDs. These areas experience intense snowfall and heavy rainfall events, which are critical for hydrological cycles and glacier accumulation.

Table 1. Overview of common atmospheric forecasting models used for weather prediction.

Model Name	Developed By	Global Grid Resolution	Forecast Range	Specific Strength/Accuracy
Global Forecast System (GFS)	National Centers for Environmental Prediction (NCEP), USA	~13 km	Up to 16 days	Moderate accuracy in global-scale prediction; widely used operational model
European Centre for Medium-Range Weather Forecasts (ECMWF)	European Union (EU)	~9 km	Up to 10 days	High accuracy in mid-latitude systems and extratropical cyclones
Weather Research and Forecasting (WRF) Model	National Center for Atmospheric Research (NCAR), USA	3–5 km	3–5 days	High-resolution regional forecasts; effective in complex terrain
Global Ensemble Forecast System (GEFS)	National Centers for Environmental Prediction (NCEP), USA	~25–50 km (ensemble mean)	Up to 16 days	Ensemble spread enables uncertainty quantification

Global Environmental Multiscale Model (GEM)	Canadian Meteorological Centre (CMC), Canada	~25 km	Up to 7 days	Effective over polar and mid-latitude regions
Unified Model (UM)	UK Met Office, United Kingdom	~17 km	Up to 10 days	Strong simulation capability for tropical and subtropical regions

- Uttarakhand, although farther east, also endures substantial precipitation and snow during March WDs. These disturbances significantly influence the Ganga River basin hydrology and increase landslide susceptibility.
- Punjab and Haryana, situated in the Indo-Gangetic plain, are agriculturally intensive states where WD-induced rainfall is crucial for rabi crops such as wheat. However, excess precipitation or hail events can negatively impact crop health and yield.
- Delhi, a densely populated urban area, frequently experiences abrupt temperature drops, rainfall, and thunderstorms during strong WD events in March, affecting air quality and urban infrastructure.
- Northern Rajasthan (e.g., Ganganagar, Hanumangarh) and northern Uttar Pradesh (e.g., Saharanpur, Muzaffarnagar, Bijnor, and Lakhimpur Kheri), typically arid or semi-arid, experience rare yet impactful rainfall during Western Disturbances, often leading to localized flooding or dust storms due to sudden atmospheric instability.

By covering this climatically diverse terrain, the study offers a comprehensive view of WD-induced weather variability. The selection of states enhances the scientific value of the study by allowing multi-terrain model validation and demonstrating the WRF model's robustness in capturing complex atmospheric interactions across elevations and land-use types.

DATASET

This study utilizes multiple datasets to analyze the Western Disturbance (WD) event, including numerical model outputs, satellite observations, and reanalysis data. Each data source provides complementary strengths for understanding mesoscale atmospheric processes over the northwestern Indian region.

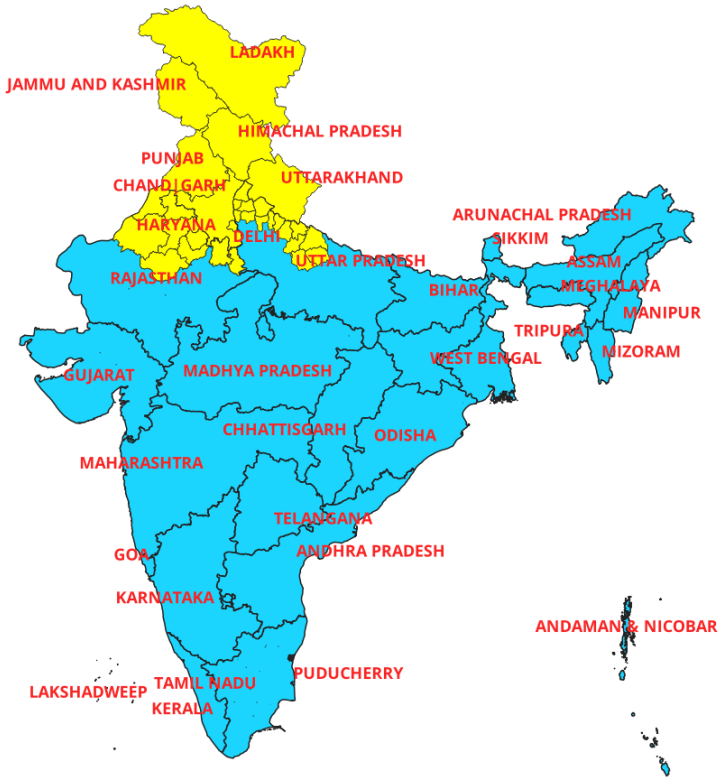

Figure 1. Study area map highlighting regions affected by Western Disturbances during March events.
The highlighted states and northern districts were selected based on climatological relevance. Administrative boundaries are based on Survey of India data (https://onlinemaps.surveyofindia.gov.in/Digital_Product_Show.aspx) The map was generated using QGIS for spatial visualization.

WRF Model Simulated Output

The Weather Research and Forecasting (WRF) model version 4.2.2 was used to generate a three-day forecast for 24–25 March 2023. Simulations were conducted at a high spatial resolution of 5 km×5 km with 3-hourly temporal granularity. The model employs the ARW core and uses GFS input data for initialization. The parameters extracted from the WRF simulations include:

- *U10 and V10:* Zonal and meridional components of 10-m wind speed, essential for assessing wind direction and magnitude.
- *Snow:* Solid precipitation, important for understanding orographic effects during WDs.
- *Rain:* Liquid precipitation; although the WRF model simulates this, previous studies indicate limitations in its accuracy for rain events.
- *Surface Pressure:* Useful for identifying synoptic-scale systems such as low-pressure centers.
- *Outgoing Longwave Radiation (OLR):* Serves as a proxy for cloud cover and convective activity.

These outputs were analyzed through visualizations and statistical comparisons with observational datasets.

Reanalysis Data: ERA-5

The ERA-5 reanalysis dataset, provided by the European Centre for Medium-Range Weather Forecasts (ECMWF), offers global atmospheric data at 25 km×25 km spatial resolution and 1-hour temporal intervals. It includes 60 vertical levels up to 0.1 hype. ERA-5 is widely recognized for its consistency and has been used here to benchmark WRF model outputs.

Satellite Observations

- *PERSIANN (Precipitation estimation from remotely sensed information using artificial neural networks):* Provides 6-hourly rainfall estimates at a spatial resolution of 4 km×4 km. It integrates

geostationary satellite imagery and ANN algorithms. PERSIANN Information: https://chrsdata.eng.uci.edu/

- *INSAT-3D:* Data obtained from the Meteorological and Oceanographic Satellite Data Archival Centre (MOSDAC) for parameters such as:
  - *Rainfall and Snowfall:* Daily resolution at 4 km×4 km spatial scale.
  - *OLR:* Daily observations at 8 km×8 km resolution.

Each dataset differs in spatial and temporal resolution, with WRF offering the finest resolution, followed by satellite products and reanalysis data. Table 2 summarizes the datasets and their key characteristics.

METHODOLOGY

WRF Model Setup

This study utilized the Advanced Research WRF (ARW) model (Figure 2) version 4.2.2 to simulate the Western Disturbance (WD) event of 24–25 March 2023, selected due to its high impact across northwestern India, including unusual convective rainfall in semi-arid regions. The simulation was validated using ERA5, PERSIANN-CDR, and MOSDAC satellite datasets.

Model Setup and Configuration

The WRF model was configured with a single domain encompassing the northwestern Indian region, with a high spatial resolution of 5 km×5 km to better resolve mesoscale features associated with WDs.

Table 2. Summary of datasets used in the study.

Data Source	Parameters Included	Resolution	Temporal Frequency
WRF Model	u10, v10, snow, rain, surface pressure, OLR	5 km×5 km	3-hourly
ERA-5	Precipitation, snow, wind, cloud cover, pressure	25 km×25 km	1-hourly
PERSIANN	Rainfall	4 km×4 km	6-hourly
INSAT-3D	Rain, snow (4 km); OLR (8 km)	Daily	Daily

The domain included the states of Jammu & Kashmir, Himachal Pradesh, Uttarakhand, Punjab, Haryana, northern Rajasthan, and northern Uttar Pradesh.

The model was initialized and run using WPS modules (Geogrid, Ungrib, Metgrid), followed by real.exe and wrf.exe. The validation period matched the event duration (24–25 March 2023). No explicit bias correction was applied; however, all comparison datasets were interpolated to the WRF grid.

Analysis Methods

To assess the model's performance, both qualitative and quantitative analyses were conducted in a structured manner.

Qualitative Analysis

Visual comparisons were made between WRF output and observational/reanalysis datasets through:

- Contour plots of spatial distributions (rainfall, wind, Total Cloud Cover, etc.).
- Time-series graphs of daily and hourly values.

This helped assess the temporal evolution and spatial accuracy of the simulation without purely relying on numerical scores. Table 3 shows the WRF model configuration.

Table 3. WRF model configuration.

Component	Details
Model Version	WRF-ARW v4.2.2
Simulation Period	24–25 March 2023
Input Data	GFS 0.25° Forecast Data

Grid Dimensions (W-E, S-N)	350×319
Vertical Layers (bottom-up)	32
Spatial Resolution	5 km×5 km
Map Projection	Mercator
Physics Parameterizations	Microphysics: Thompson aerosol-aware (MP_PHYSICS); PBL: MYNN (BL_PBL_PHYSICS); Radiation: RRTMG (RA_LW_PHYSICS, RA_SW_PHYSICS); Cumulus: None (CU_PHYSICS, explicit convection)
Output Variables	Rainfall, Wind (u10, v10), OLR, Total Cloud Cover, Surface Pressure, Snow

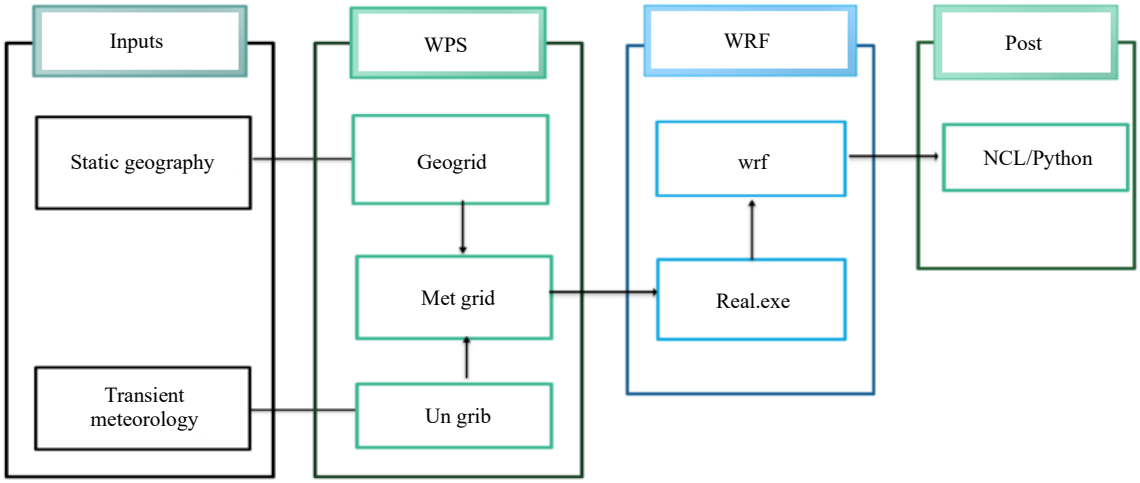

Figure 2. Workflow of the WRF model as implemented in this study.

Quantitative Analysis

To statistically evaluate the model's accuracy, the following metrics were used:

- Root Mean Square Error (RMSE).
- Mean Square Error (MSE).
- Pearson Correlation Coefficient (r),

These metrics were calculated between WRF outputs and ERA5 or satellite data for variables like rainfall, OLR, and surface wind speed. Below are the respective formulae:

Equation 1: RMSE

$$RMSE = \sqrt{\frac{1}{n}\sum_{i=1}^{n}(P_i - O_i)^2}$$

Equation 2: MSE

$$MSE = \frac{1}{n}\sum_{i=1}^{n}(P_i - O_i)^2$$

Equation 3: Coefficient

$$r = \frac{\sum(P_i-\bar{P})(O_i-\bar{O})}{\sqrt{\sum(P_i-\bar{P})^2}\ \sqrt{\sum(O_i-\bar{O})^2}}$$

Where P_i and O_i are predicted and observed values, respectively, and n is the number of observations.

RESULTS

Qualitative Analysis

Satellite-Derived Observations

Figures 3 and 4 show rainfall from PERSIANN and outgoing longwave radiation (OLR) from MOSDAC, respectively, on 24 March 2023. Rainfall was notably observed over Jammu & Kashmir and Himachal Pradesh. The OLR plot indicates reduced values over high cloud-cover regions, confirming cloud development associated with the Western Disturbance (WD).

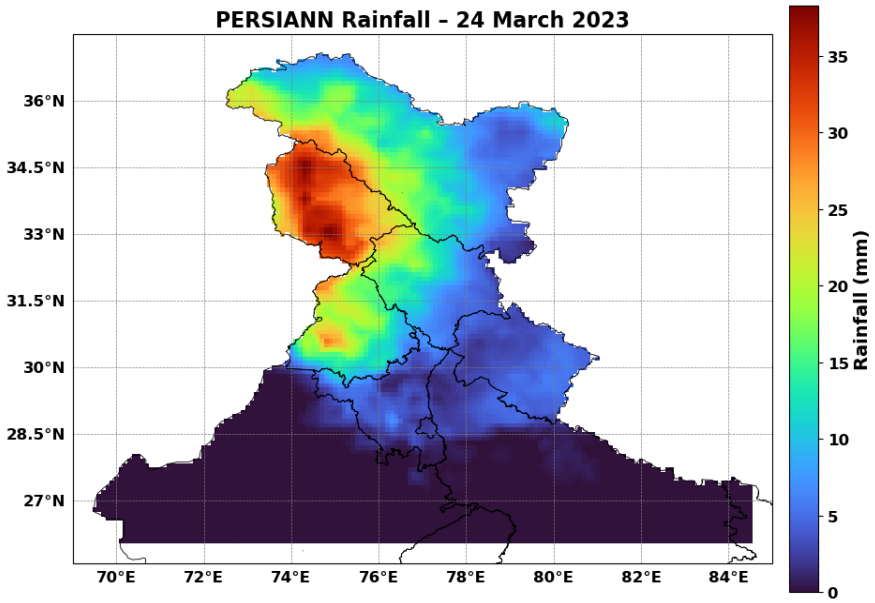

Figure 3. Rainfall distribution (mm) on 24 March 2023 derived from PERSIANN satellite data.

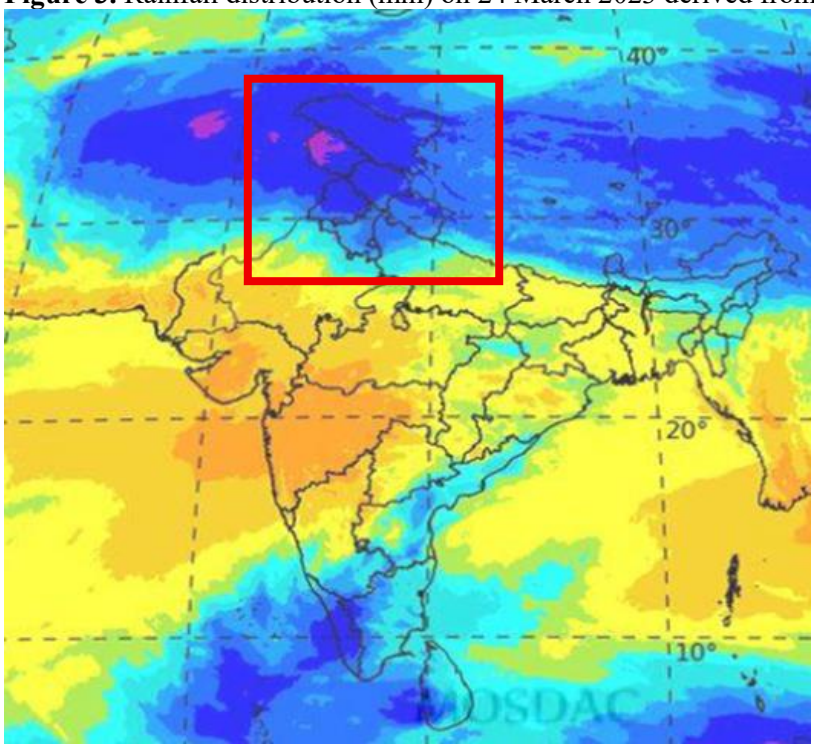

Figure 4. Outgoing Longwave Radiation (OLR) from MOSDAC on 24 March 2023 (Screenshot).

WRF Model vs. ERA5 Reanalysis

WRF simulations (Figures 5–10) demonstrate strong agreement with ERA5 data for most parameters:

- *Rainfall (Figure 5):* WRF captured the spatial trend, although it underestimated intensity over Indian territory.
- *Snowfall (Figure 6):* Consistent spatial distribution and peak values (~60 mm in Himachal Pradesh) between model and ERA5.
- *Surface Pressure (Figure 7):* Highest pressure zones are accurately identified over Punjab and Haryana.
- *Wind Fields (U10 and V10) (Figures 8 and 9):* Wind direction and magnitude evolution aligned well with reanalysis.
- *Cloud Cover and OLR (Figure 10):* Spatial anti-correlation observed, validating WRF's radiative parameterization.

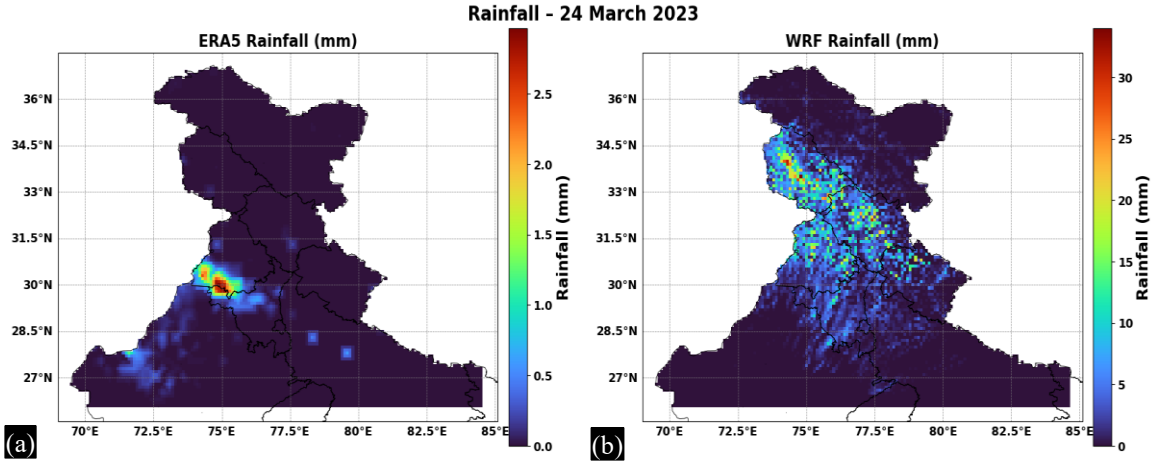

Figure 5. (a and b) ERA5 rainfall (mm) (hourly intervals) and WRF rainfall (mm) (6-hourly intervals) on 24 March 2023.

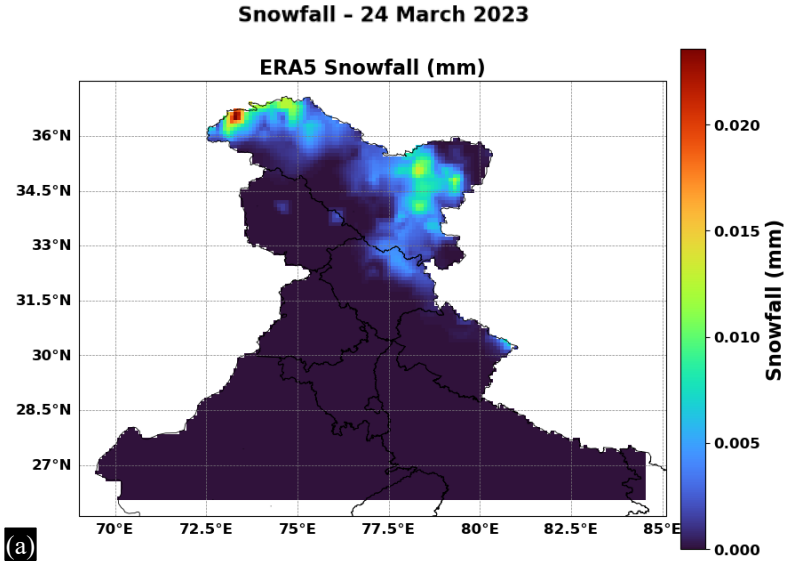

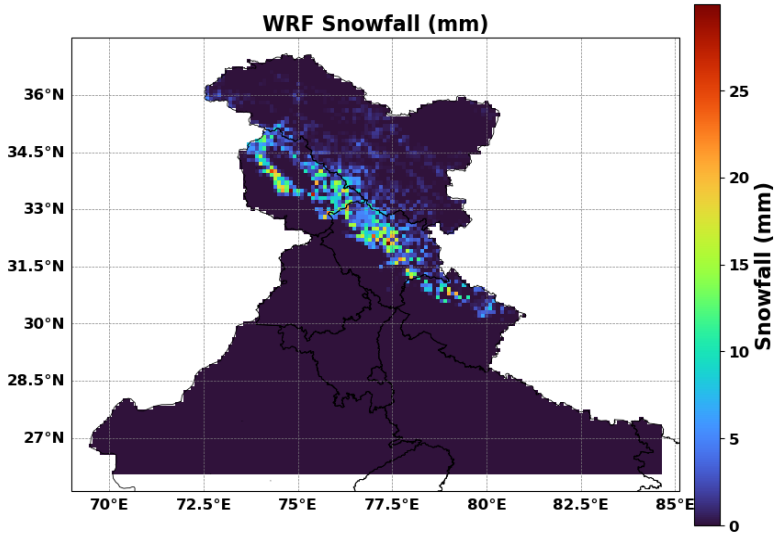

Figure 6. (a and b) ERA5 Snowfall (mm) (hourly intervals) and WRF Snowfall (mm) (6-hourly intervals) on 24 March 2023.

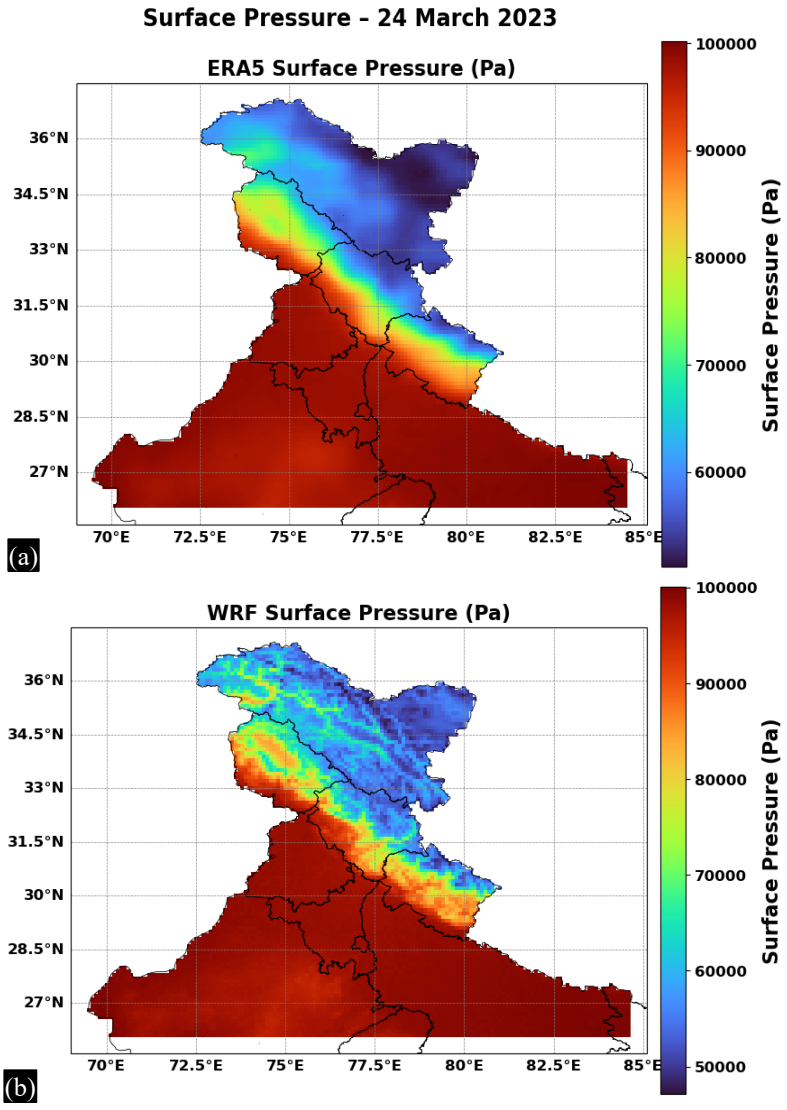

Figure 7. (a and b) ERA5 surface pressure (Pa) (hourly intervals) and WRF surface pressure (Pa) (6-hourly intervals) on 24 March 2023.

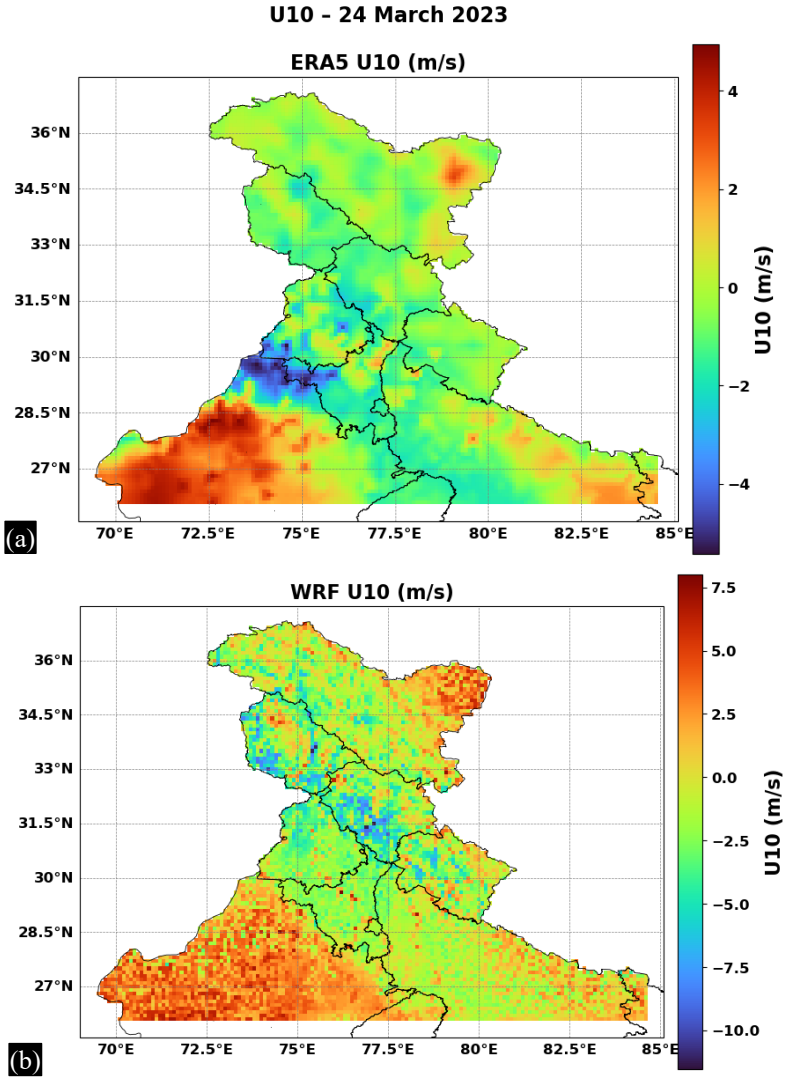

Figure 8. (a and b) ERA5 U10 (m/s) (hourly intervals) and WRF U10 (m/s) (6-hourly intervals) on 24 March 2023.

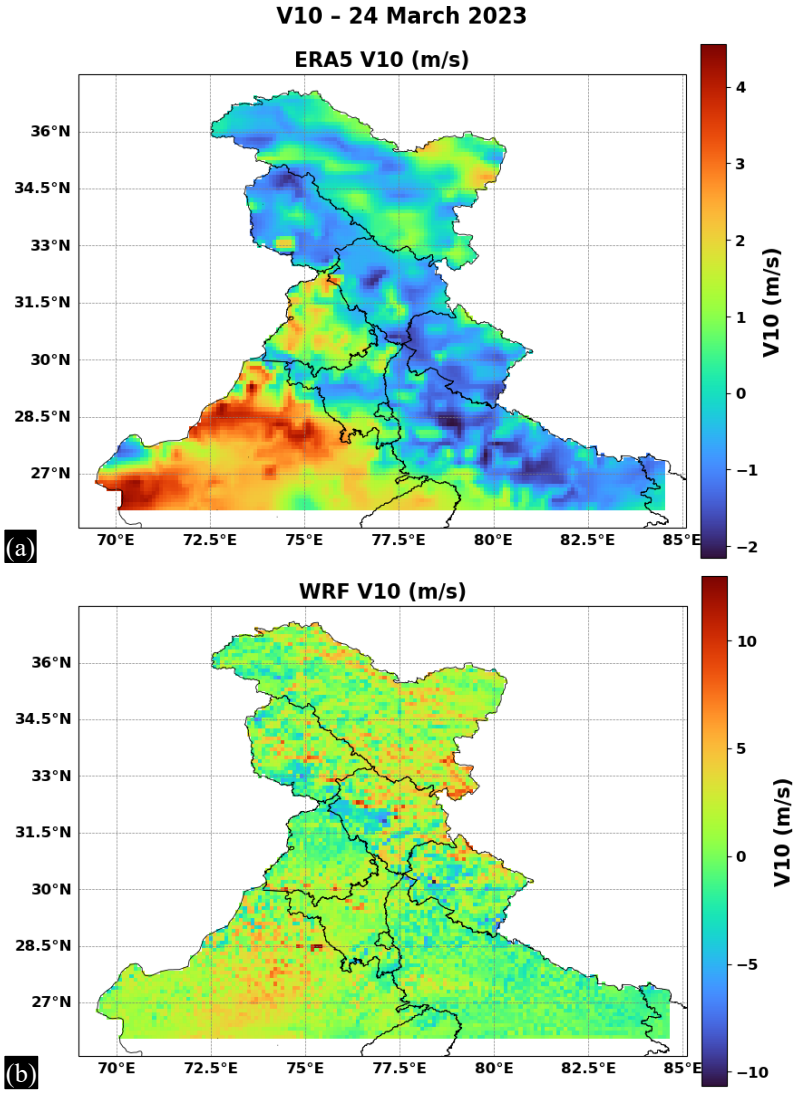

Figure 9. (a and b) ERA5 V10 (m/s) (hourly intervals) and WRF V10 (m/s) (6-hourly intervals) on 24 March 2023.

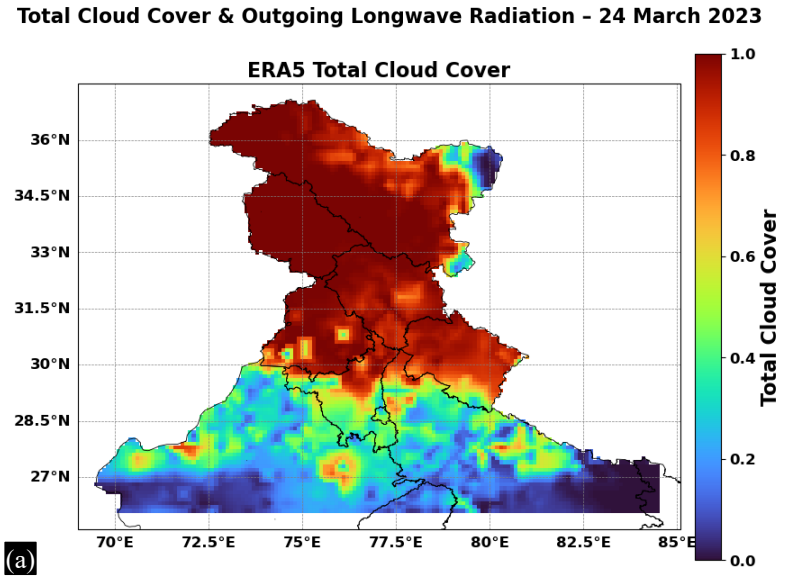

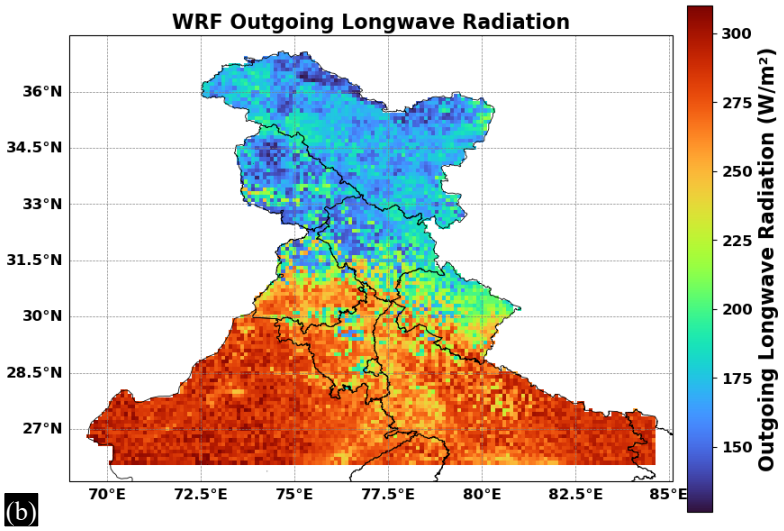

Figure 10. (a and b) ERA5 total cloud cover (hourly intervals) and WRF outgoing longwave radiation (W/m²) (6-hourly intervals) on 24 March 2023.

Spatial Evolution on 25 March

Figures 11–16 illustrate results for 25 March 2023. Notably:

- Rainfall shifted slightly eastward, affecting Jammu & Kashmir, Himachal Pradesh, and Uttarakhand.
- Snowfall peaked across central Himachal Pradesh.
- Wind magnitude increased slightly, with a persistent inverse relationship with snowfall.

Comparison with INSAT-3D Observations

Figures 17–22 present satellite-derived observations from INSAT-3D for March 25, 2023, and their comparison with WRF model outputs. Rainfall plots (Figures 17 and 18) confirm that precipitation was primarily localized over Jammu & Kashmir and Himachal Pradesh, with moderate intensity. WRF captured this spatial pattern but underestimated intensity in central Himachal Pradesh.

Figure 19 OLR from INSAT-3D, demonstrating low values over regions of dense cloud cover. These patterns are consistent with WRF simulations and support the observed inverse relationship between OLR and total cloud cover.

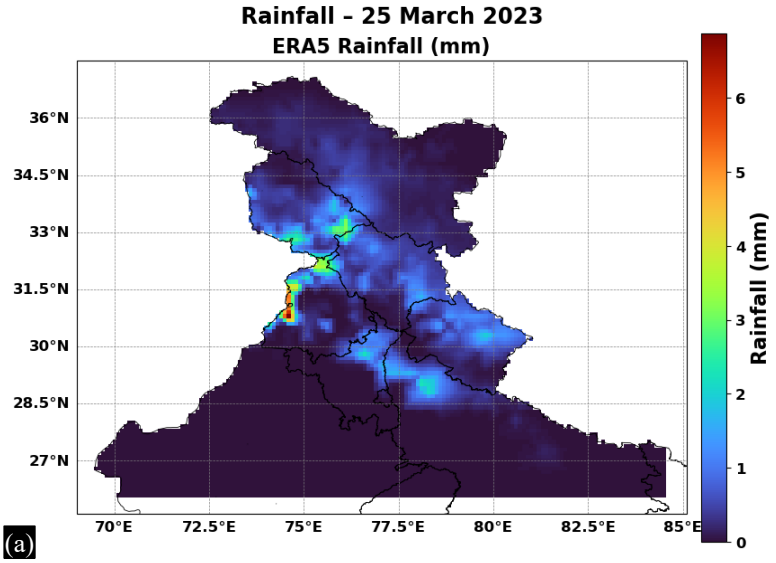

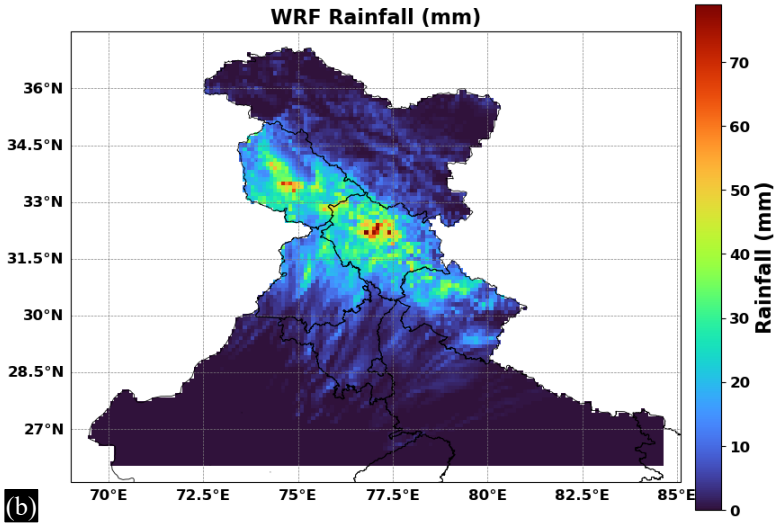

Figure 11. (a and b) ERA5 Rainfall (mm) (hourly intervals) and WRF rainfall (mm) (6-hourly intervals) on 25 March 2023.

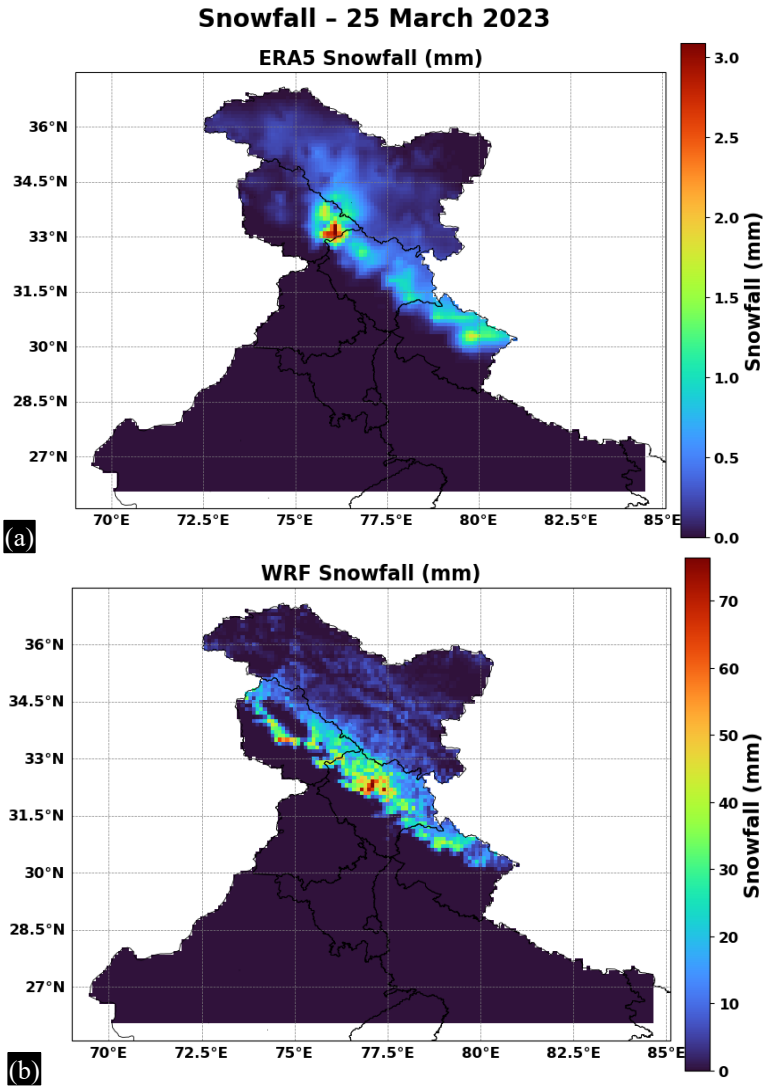

Figure 12. (a and b) ERA5 Snowfall (mm) (hourly intervals) and WRF Snowfall (mm) (6-hourly intervals) on 25 March 2023.

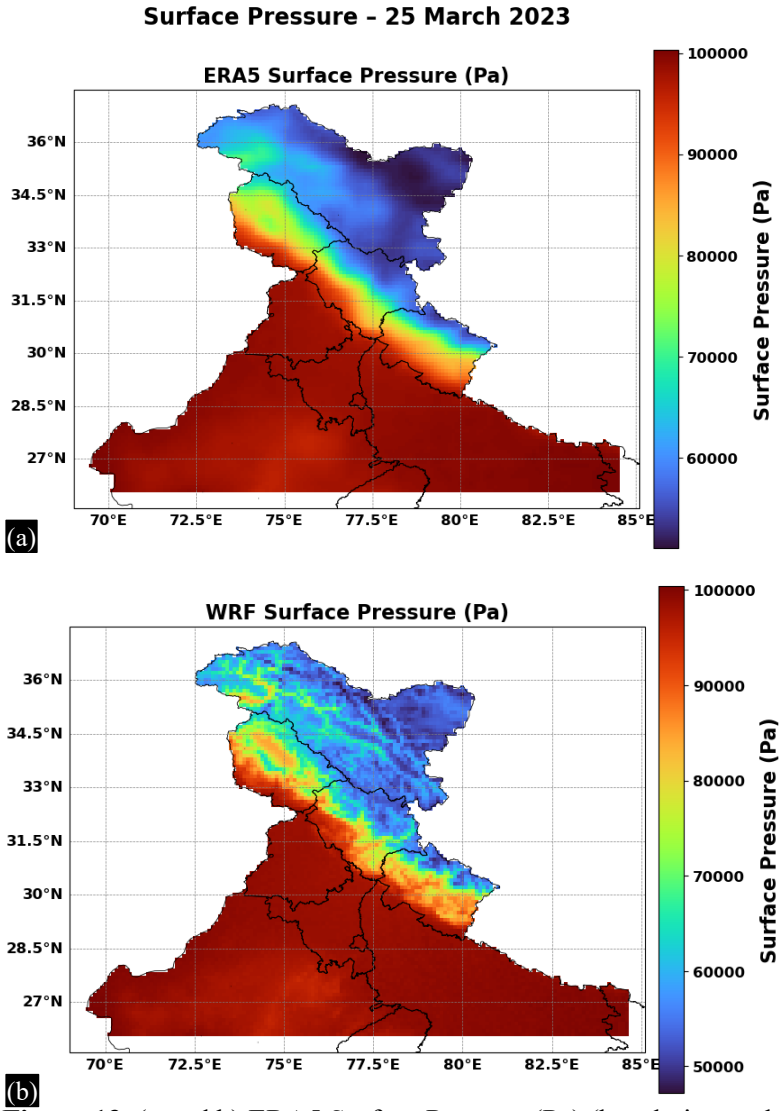

Figure 13. (a and b) ERA5 Surface Pressure (Pa) (hourly intervals) and WRF surface pressure (Pa) (6-hourly intervals) on 25 March 2023.

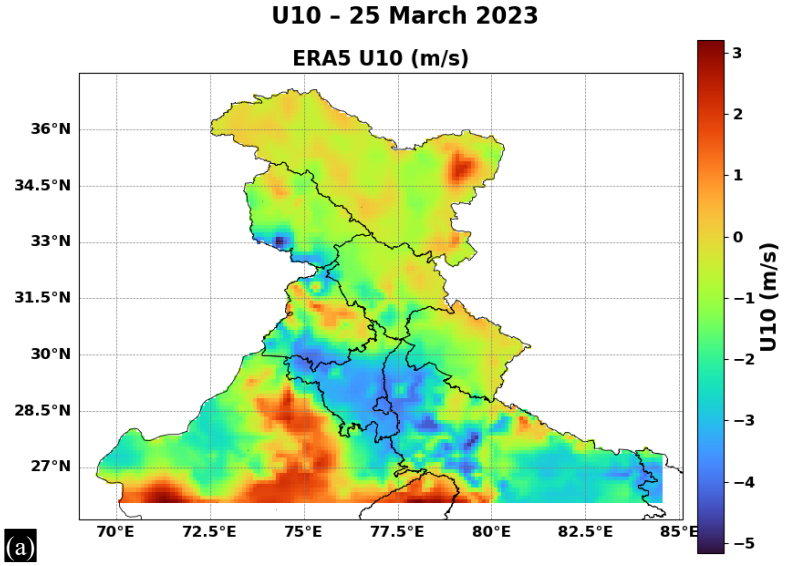

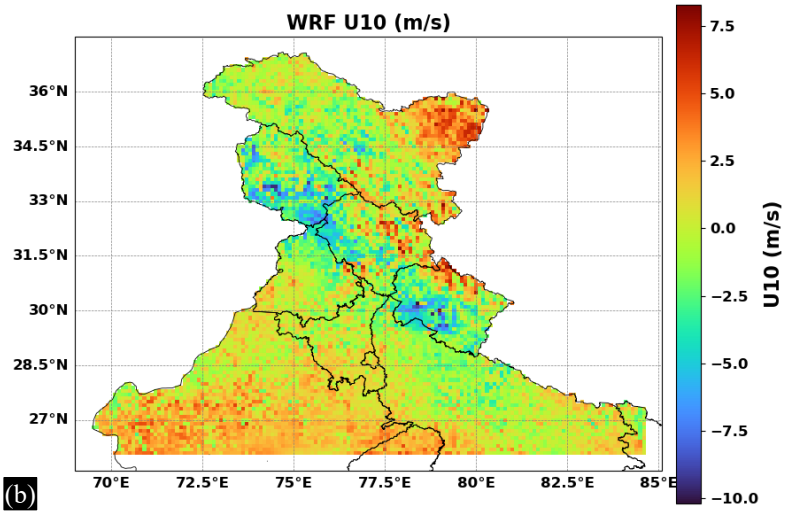

Figure 14. (a and b) ERA5 U10 (m/s) (hourly intervals) and WRF U10 (m/s) (6-hourly intervals) on 25 March 2023.

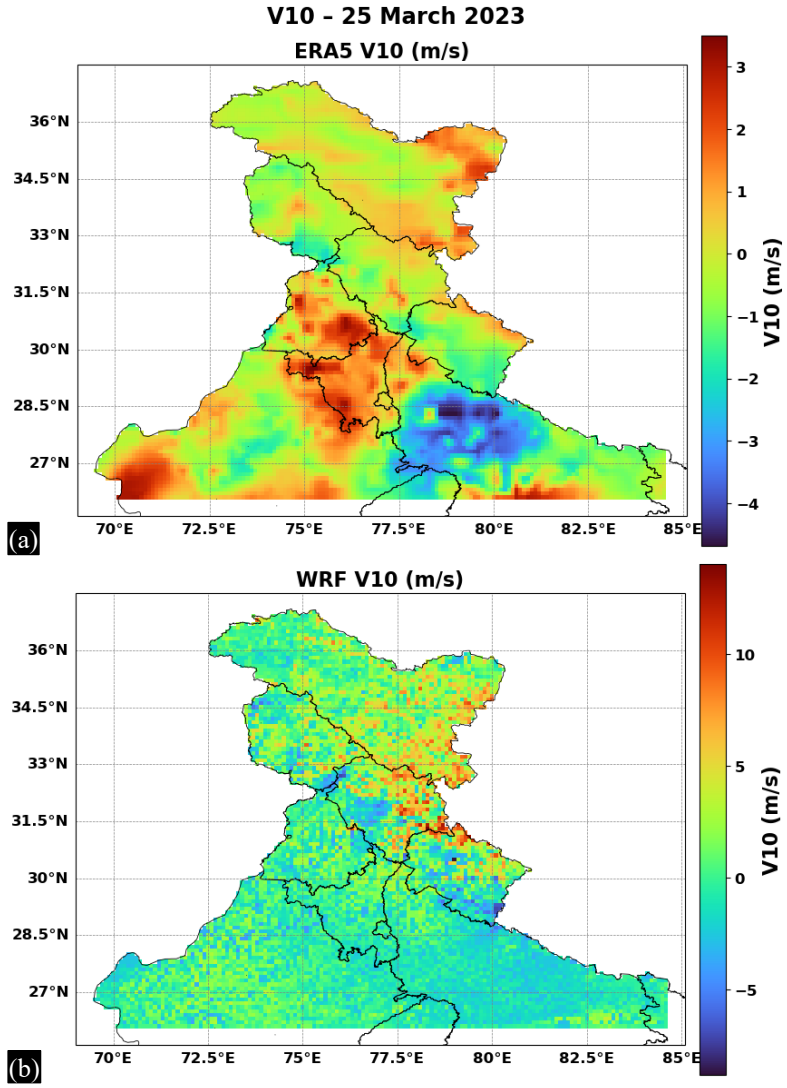

Figure 15. (a and b) ERA5 V10 (m/s) (hourly intervals) and WRF V10 (m/s) (6-hourly intervals) on 25 March 2023.

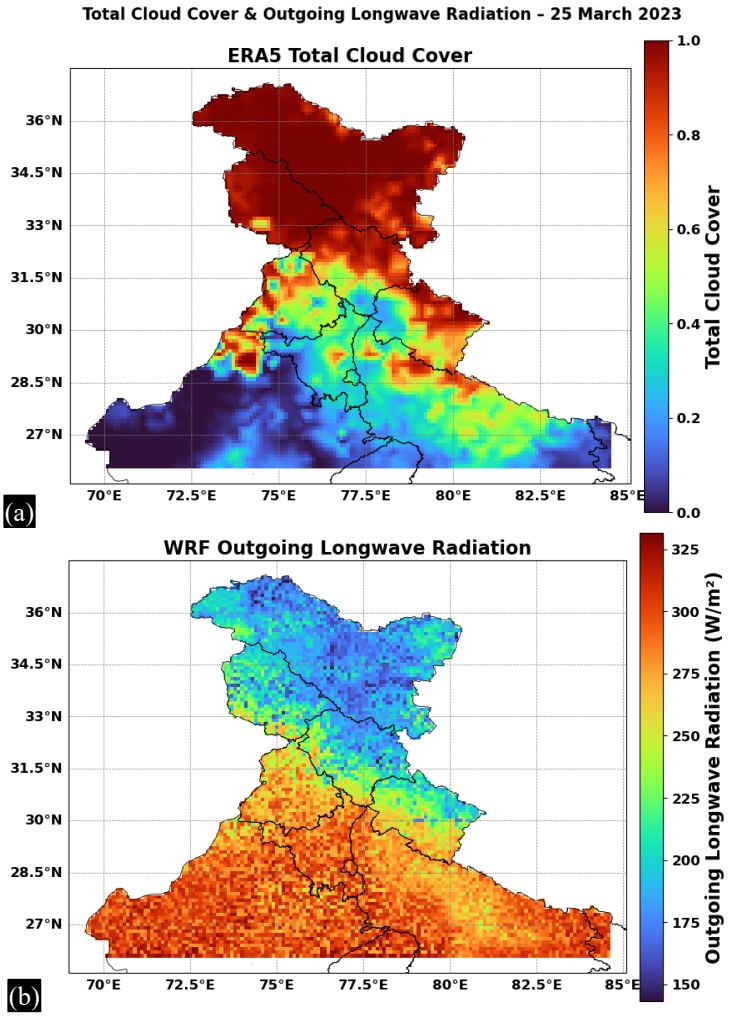

Figure 16. (a and b) ERA5 total cloud cover (hourly intervals) and WRF outgoing longwave radiation (W/m²) (6-hourly intervals) on 25 March 2023.

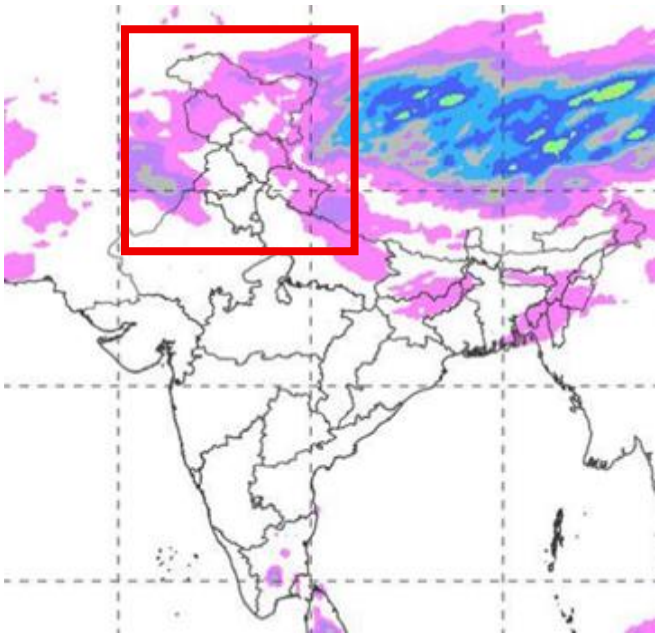

Figure 17. INSAT-3D observed rainfall (mm) on 25 March 2023 (screenshot).

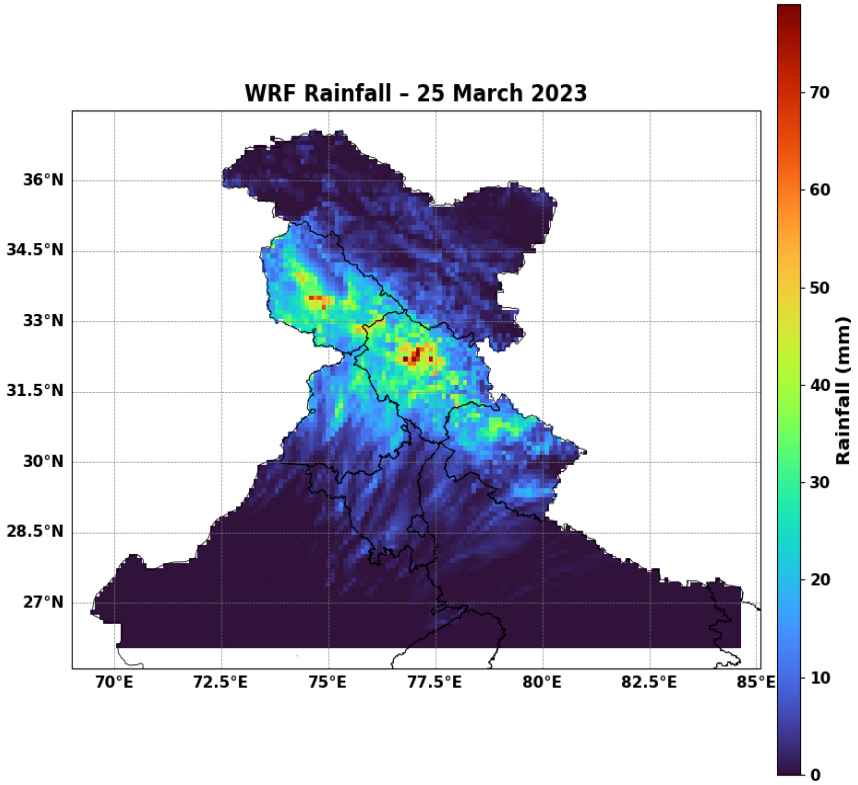

Figure 18. WRF Rainfall (mm) 25 March 2023.

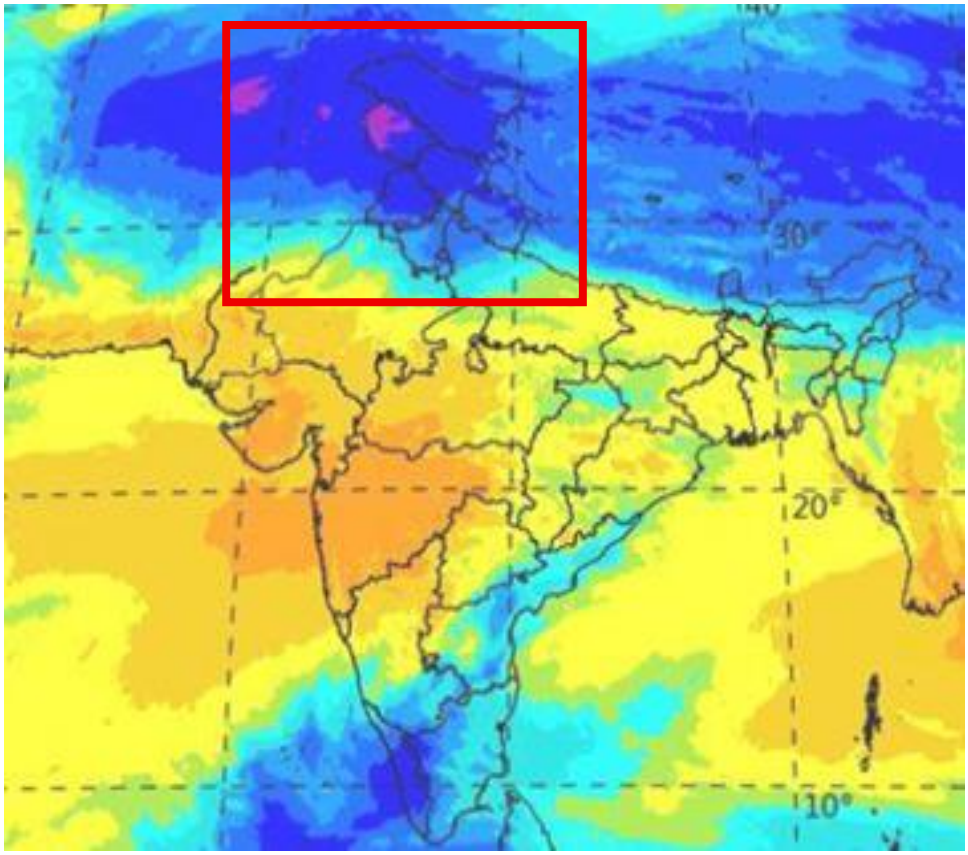

Figure 19. INSAT-3D Outgoing Longwave Radiation (OLR) (W/m²) for 25 March 2023 (Screenshot).

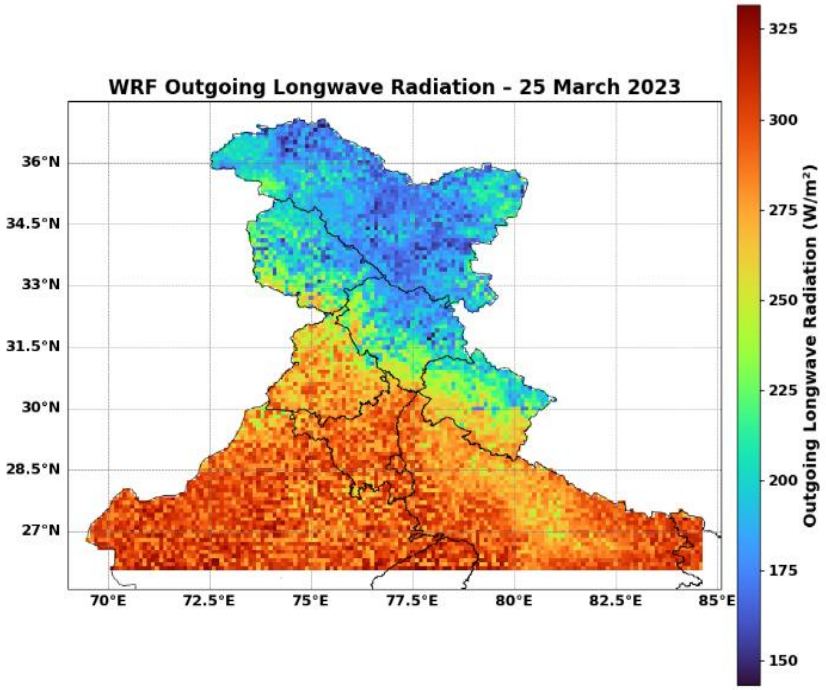

Figure 20. WRF outgoing longwave radiation 25 March 2023 (W/m²).

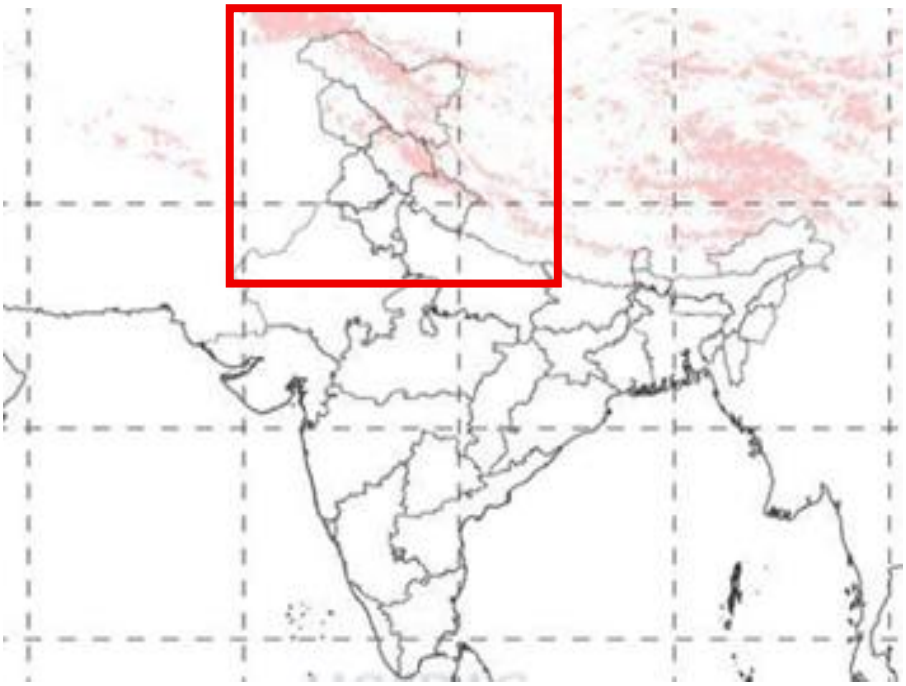

Figure 21. INSAT-3D Snowfall (mm) 25 March 2023 (Screenshot).

Snowfall distributions align well with model output, confirming snowfall occurrence in the higher altitudes of Himachal Pradesh and Uttarakhand (Figures 21 and 22). However, intensity estimates varied, likely due to resolution differences between the model and satellite datasets.

Time-Series Analysis

Figures 23–28 provide temporal comparisons of key parameters:

- *Snowfall (Figure 23):* WRF and ERA5 show similar diurnal trends with a peak on 24 March, a sharp decline by 25 March.

- *OLR vs. Cloud Cover (Figure 24):* Inverse correlation evident, with increased cloud cover lowering OLR.
- *Surface Pressure (Figure 25):* High correlation supports the model's strength in synoptic-scale pressure systems.
- *Wind Components (Figures 26 and 27):* U10 and V10 values consistent across model and reanalysis.
- *Snowfall vs. Wind (Figure 28):* Snowfall increases with decreased wind speed, indicating suppressed advection during the active WD phase.

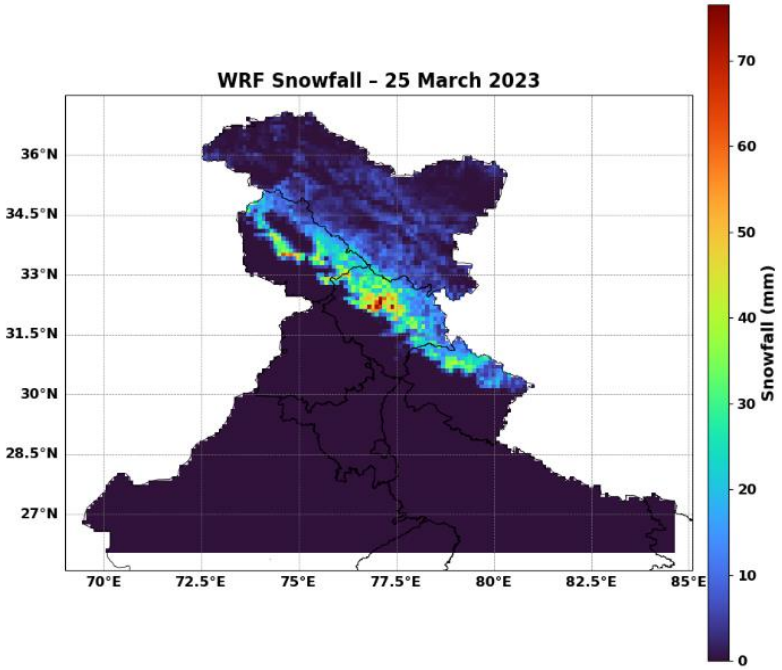

Figure 22. WRF Snowfall (mm) 25 March 2023.

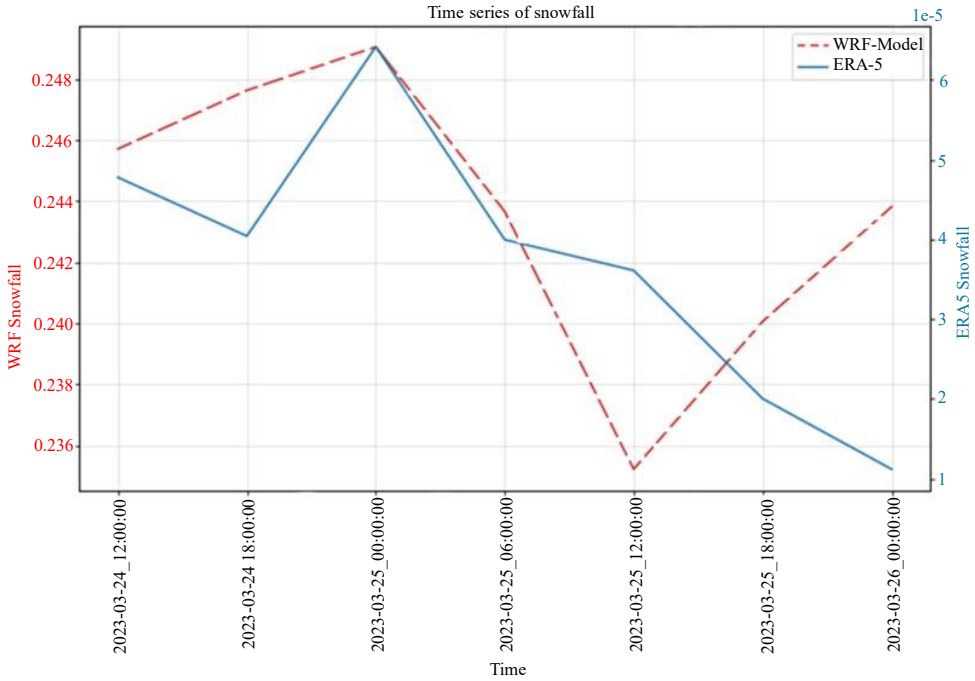

Figure 23. Time series of Snowfall (mm) comparing WRF and ERA5 from 24–25 March 2023.

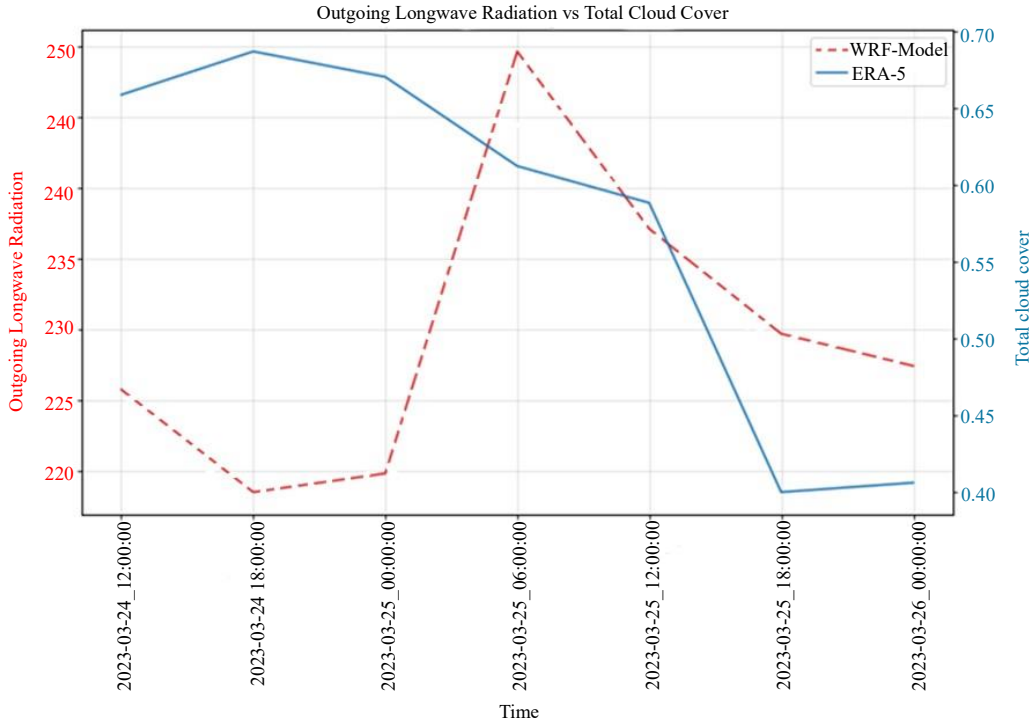

Figure 24. Comparative time-series showing inverse relationship between WRF-modeled OLR and ERA5 total cloud cover.

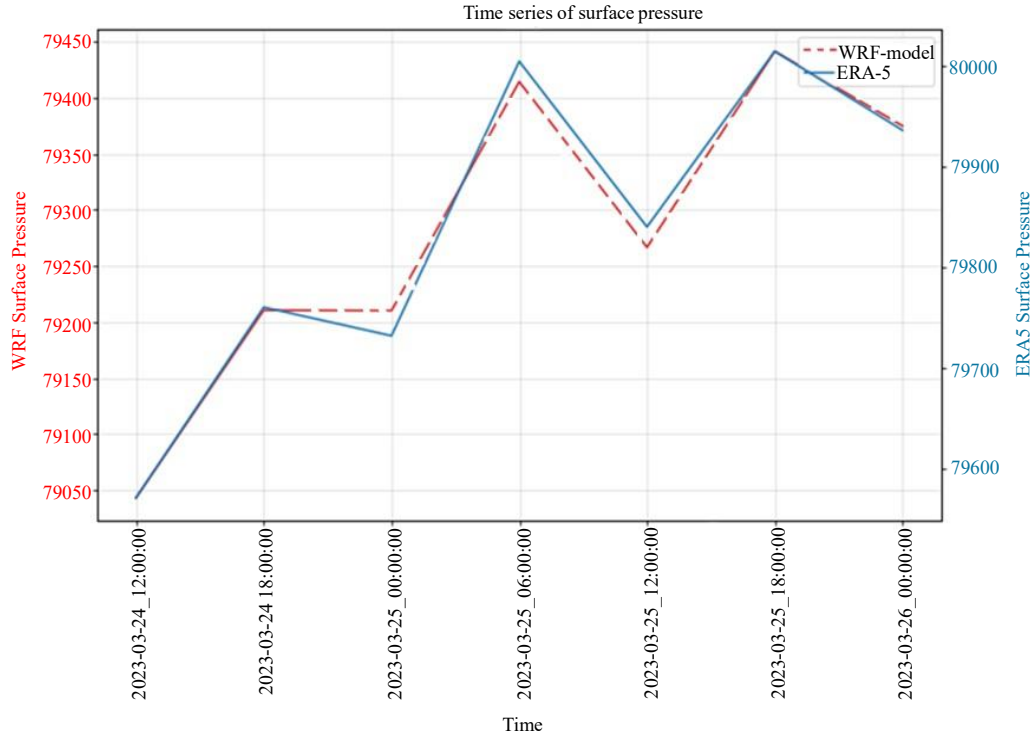

Figure 25. Time series of Surface Pressure from WRF and ERA5 showing consistent trends across 24–25 March.

QUANTITATIVE EVALUATION

To objectively assess the WRF model's performance during the 24–25 March 2023 Western Disturbance (WD), statistical metrics: Root Mean Square Error (RMSE), Mean Square Error (MSE),

and Pearson correlation coefficient (r), were computed for rainfall, snowfall, and 10-m wind components (U10 and V10) against ERA5 reanalysis data.

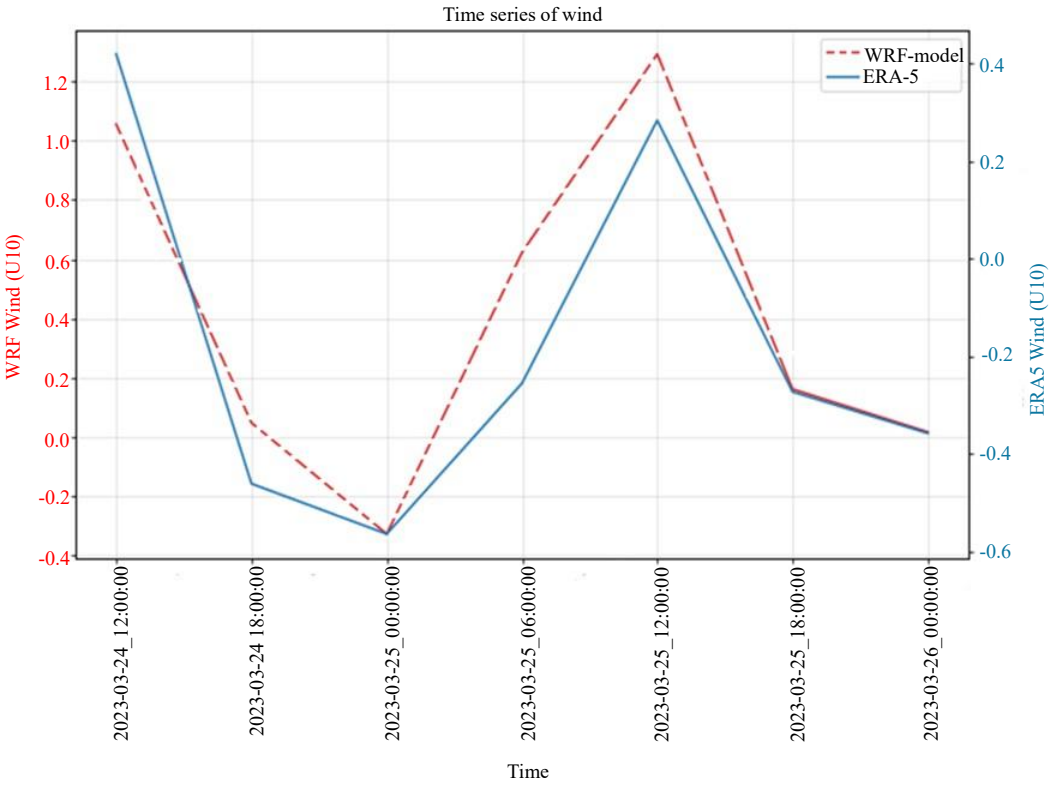

Figure 26. Wind Speed (U10) time-series comparison.

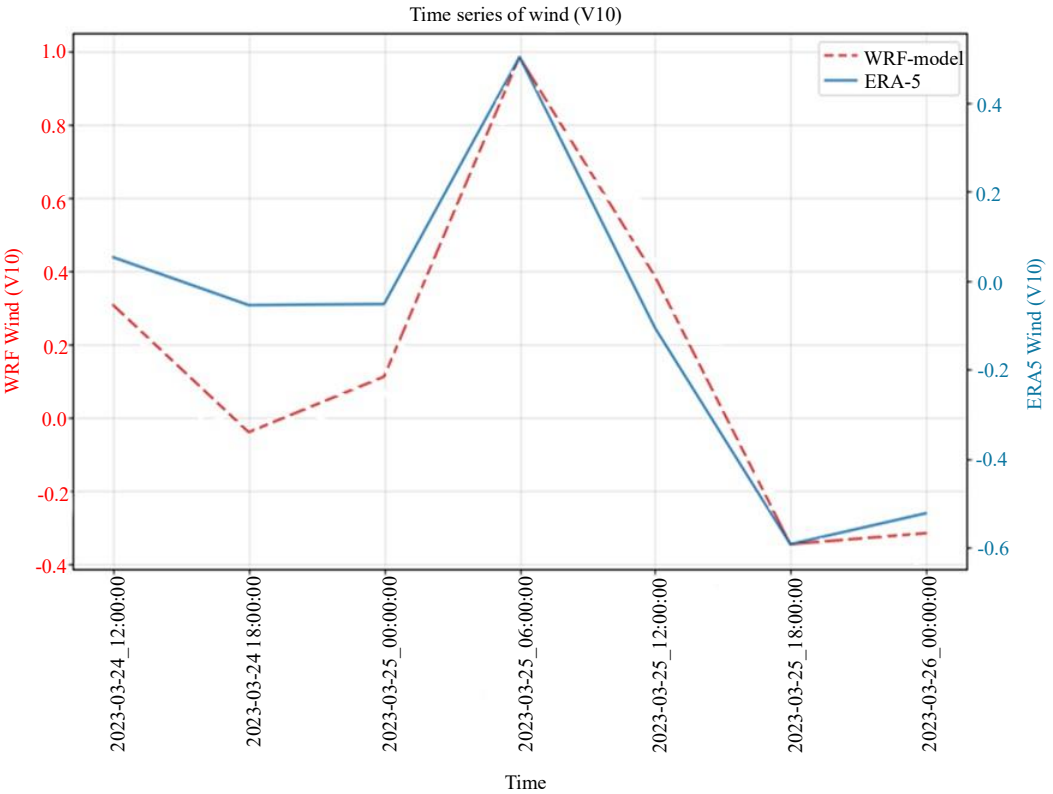

Figure 27. Wind Speed (V10) time-series confirming directional dynamics between WRF and ERA5.

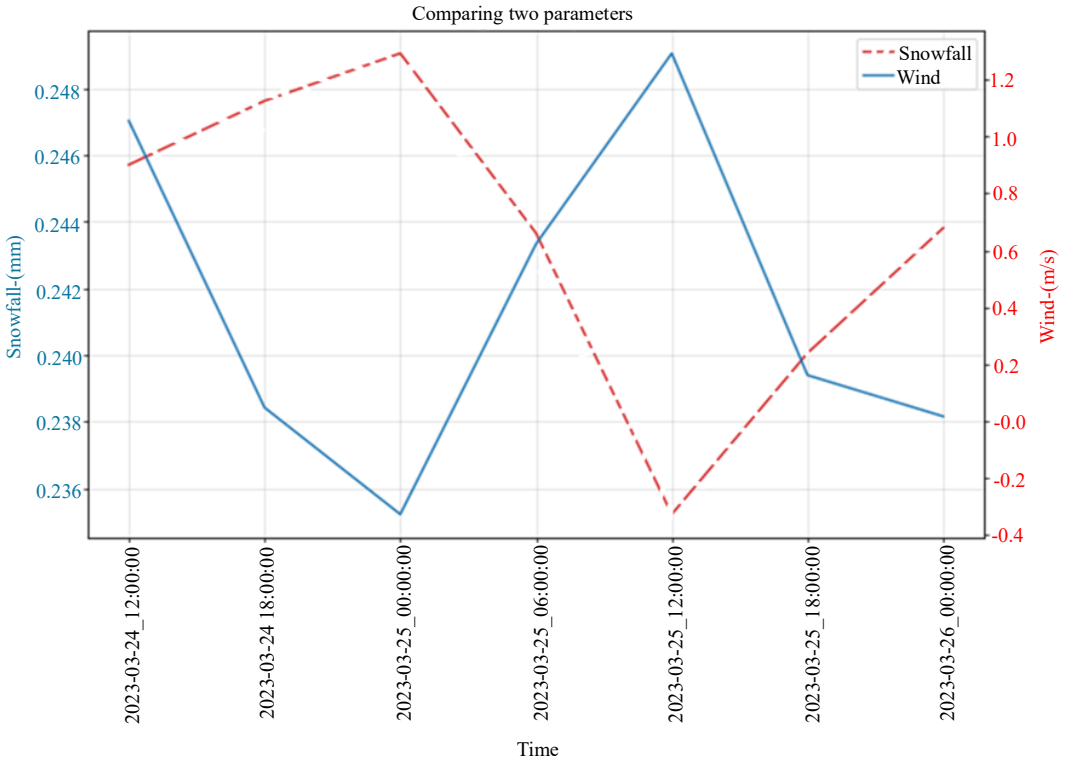

Figure 28. Time series analysis highlighting the inverse relationship between Snowfall (mm) and Wind Speed (U10) during event.

Table 4. Performance metrics for WRF model compared to ERA5 reanalysis (24–25 March 2023).

Variable	RMSE	MSE	Correlation (r)
RAINNC	4.46	19.89	0.41
SNOWNC	1.40	1.98	0.78
U10	0.63	0.40	0.91
V10	0.30	0.09	0.89

The results (Table 4) indicate that:

- Rainfall (RAINNC) exhibited the highest RMSE (4.46 mm) and the lowest correlation (r=0.42), confirming that the model underperforms in simulating rainfall, likely due to microphysics limitations and complex terrain interaction.
- Snowfall (SNOWNC) performed considerably better (RMSE=1.40 mm, r=0.78), highlighting the model's strength in capturing solid precipitation over orographic regions.
- Wind speed components (U10, V10) were accurately simulated, with low RMSEs (0.63 and 0.30 m/s, respectively) and strong correlations (r>0.80), demonstrating reliable representation of wind dynamics.

Time-series graphs in Figures 23–28 further validate model accuracy. Notably, wind speed and snowfall exhibit an inverse relationship, and OLR inversely correlates with total cloud cover, consistent with theoretical expectations.

While the model reliably simulates wind and snowfall, it significantly underestimates rainfall intensity and distribution. This could be attributed to limitations in microphysical parameterization and the absence of cumulus schemes, which may restrict the representation of convective precipitation despite the high spatial resolution.

DISCUSSION

The performance of the WRF model during the 24–25 March 2023 Western Disturbance reveals important insights into its capabilities and limitations, particularly in a complex mountainous environment. The WRF model significantly underestimates rainfall intensity and distribution compared to both ERA5 and satellite-based observations. This shortfall can be primarily attributed to the limitations of the microphysics scheme, which may not adequately represent convective processes and hydrometeor interaction over varied terrain [4, 5]. Additionally, the model was run without a cumulus parameterization scheme due to its high-resolution 5 km grid, which, while suitable for explicit convection in theory, often leads to weakened convective activity in practice, especially in orographically influenced regions [12].

The Himalayas present a significant modeling challenge. Orographic lifting, valley wind effects, and temperature inversions are difficult to simulate accurately. These features lead to localized enhancement of precipitation that may be missed even in high-resolution simulations. The model's terrain-following vertical coordinate system and static land-use assumptions may further reduce its ability to represent localized convective and microphysical processes.

These findings are consistent with prior research. Patil and Kumar noted similar rainfall underestimation in WD simulations using WRF over North India, attributing the issue to parameterization choices [5]. Chawla *et al*. also observed discrepancies in simulating extreme rainfall events in the upper Ganga basin [4]. The better simulation of wind and snowfall seen in our study aligns with Dimri and Chevuturi [2], who highlighted the model's strengths in representing large-scale dynamical fields under Western Disturbance conditions.

Despite rainfall biases, the WRF model effectively captures snowfall patterns and wind dynamics. The observed inverse relationship between total cloud cover (TCC) and outgoing longwave radiation (OLR), and between snowfall and U10 wind, reflects the model's reasonable representation of radiative processes and advection-suppressed snow events. These patterns are physically consistent with mid-latitude WD systems and highlight the model's utility in forecasting wind-driven snow conditions and cold air dynamics.

Recommendations for Future Improvement

To enhance simulation accuracy in future studies, the following improvements are recommended:

- Test multiple microphysics schemes (e.g., Thompson, Morrison) to evaluate rainfall sensitivity.
- Explore cumulus parameterization sensitivity, even at convection-permitting scales, particularly in transition zones like NW India.
- Incorporate ensemble modeling to capture uncertainty in initial conditions and model physics.
- Apply bias correction techniques using ground-based or satellite data.
- Increase land-surface resolution or use dynamic vegetation modules to improve terrain and surface-atmosphere interactions.

These strategies may reduce model biases and better resolve precipitation variability over the Himalayan and adjoining regions, ultimately aiding disaster risk reduction, agricultural decision-making, and early warning systems.

CONCLUSION

This study assessed the performance of the WRF-ARW v4.2.2 model during the Western Disturbance (WD) event of 24–25 March 2023 across northwestern India, using ERA-5 reanalysis and satellite observations from PERSIANN and INSAT-3D. The model effectively captured key dynamical fields such as wind components and snowfall, but substantially underestimated rainfall amounts and distribution.

Quantitatively, the WRF Model Demonstrated

- *Strong agreement for wind:* U10 (RMSE: 0.63 m/s, r=0.91) and V10 (RMSE: 0.30 m/s, r=0.89).
- *Reliable performance for snowfall:* RMSE of 1.40 mm, r=0.78.
- *Weak performance for rainfall:* RMSE of 4.46 mm and correlation of 0.41.

These results highlight the model's strength in simulating orographically driven snow and wind patterns, but also its limitations in resolving convective rainfall under complex terrain and atmospheric conditions. Qualitative assessments revealed physically consistent meteorological relationships such as the inverse correlation between total cloud cover and outgoing longwave radiation, and between snowfall and wind speed, further supporting the model's reliability in simulating large-scale dynamics associated with WDs.

Overall, WRF shows promise for forecasting snow and wind-related extremes in mountainous regions, which is critical for disaster risk management, infrastructure resilience, and climate-sensitive sectors. However, due to significant rainfall biases, caution is advised when using its outputs for agricultural planning or hydrological modeling without prior validation. This case-specific evaluation offers useful insights into the capabilities and constraints of high-resolution regional modeling and underscores the need for context-aware configurations when applying WRF to WD scenarios.

REFERENCES

1. Dimri AP, Niyogi D, Barros AP, Ridley J, Mohanty UC, Yasunari T, Sikka DR. Western disturbances: a review. Rev Geophys. 2015 Jun; 53(2): 225–46.
2. Dimri AP, Chevuturi A. Western disturbances-an Indian meteorological perspective. Cham: Springer; 2016.
3. Shekhar MS, Chand H, Kumar S, Srinivasan K, Ganju A. Climate-change studies in the western Himalaya. Ann Glaciol. 2010 Jan; 51(54): 105–12.
4. Chawla I, Osuri KK, Mujumdar PP, Niyogi D. Assessment of the Weather Research and Forecasting (WRF) model for simulation of extreme rainfall events in the upper Ganga Basin. Hydrol Earth Syst Sci. 2018 Feb 8; 22(2): 1095–117.
5. Patil R, Pradeep Kumar P. WRF model sensitivity for simulating intense western disturbances over North West India. Model Earth Syst Environ. 2016 Jun; 2(2): 82.
6. Samantray P, Gouda KC. A review on the extreme rainfall studies in India. Nat Hazards Res. 2024 Sep 1; 4(3): 347–56.
7. Gill KK, Kaur S, Sandhu SS, Bhatt K. Western disturbances: Occurrence and impact on wheat productivity in Punjab. J Agrometeorol. 2024 Sep 1; 26(3): 339–43.
8. Al-Ruzouq R, Shanableh A, Jena R, Gibril MB, Hammouri NA, Lamghari F. Flood susceptibility mapping using a novel integration of multi-temporal sentinel-1 data and eXtreme deep learning model. Geosci Front. 2024 May 1; 15(3): 101780.
9. Sudha Rani Nalakurthi NV, Behera MR, Bhaskaran PK. Land subsidence detection using sentinel-1 interferometer and its relation with environmental drivers: a case study for coastal Mumbai city. Spat Inf Res. 2024 Dec; 32(6): 665–81.
10. Shamsuzzoha M, Shaw R, Ahamed T. Machine learning system to assess rice crop change detection from satellite-derived RGVI due to tropical cyclones using remote sensing dataset. Remote Sens Appl: Soc Environ. 2024 Aug 1; 35: 101201.
11. Srivastava A, Thakur AK, Garg RD. An assessment of the spatiotemporal dynamics and seasonal trends in NO_2 concentrations across India using advanced statistical analysis. Remote Sens Appl: Soc Environ. 2025 Jan 1; 37: 101490.
12. Yáñez-Morroni G, Gironás J, Caneo M, Delgado R, Garreaud R. Using the Weather Research and Forecasting (WRF) model for precipitation forecasting in an Andean region with complex topography. Atmosphere. 2018 Aug 2; 9(8): 304.

